

Dynamics of 1-D Chains of Magnetic Vortices in Response to Local and Global Excitations

Saswati Barman^{1,2}, Anjan Barman^{1,2}, and YoshiChika Otani^{2,3}

¹Department of Materials Science, S. N. Bose National Centre for Basic Sciences, Salt Lake, Kolkata 700098, India

²RIKEN ASI, Wako, Saitama 351-0198, Japan

³Institute for Solid State Physics, University of Tokyo, Kashiwa, Chiba 277-8581, Japan

We report the magnetic vortex dynamics of 1-D chains of nanomagnetic disks under a time-dependent magnetic field localized at one end of the chain. The transmission of the peak amplitude of the gyrotropic excitation mode of the vortex core along the chain has been actively controlled by manipulating the geometry and condition of preparation of the magnetic ground states of the chains. The transmission is maximum for direct magnetostatic coupling and identical chirality of the nanodisks with geometric asymmetry. Dynamics of the optimized system under a global excitation field has also been investigated to understand the role of magnetostatic interaction in the energy transfer under the local excitation field. The observations are particularly important for the design of fast spin logic systems and the magnonic crystals.

Index Terms—Magnetic vortex dynamics, micromagnetic simulations, nanomagnet arrays.

I. INTRODUCTION

MAGNETIC vortex has been a growing research area [1], [2] in the field of nanomagnetism and spin dynamics due to its potential applications in high density magnetic data storage, magnetic memory and magnetic logic devices. Static and dynamic properties of magnetic vortex such as magnetic susceptibility, vortex stability and gyrotropic oscillation of vortex core and excitation of spin waves under the application of time-dependent magnetic field have been studied recently [3]–[7]. Ultrafast switching of vortex cores driven by oscillating, pulsed or rotating magnetic fields or currents have also been experimentally and theoretically demonstrated towards possible applications in non-volatile memory devices [8]–[17]. When magnetic nanodisks with vortex states are arranged in dense arrays, the magnetic ground states of the constituent disks may get modified due to the long range dipolar interaction between the disks. On application of an external magnetic field or current pulse, the inter-disk interaction becomes stronger due to the formation of magnetic surface charges, which modify the dynamics significantly from that of an individual disk. The dynamical properties including the eigen frequency spectra of coupled magnetic vortices have been theoretically and experimentally investigated [18], [19]. However, the manipulation of magnetostatic interaction between elements and thereby influencing their dynamical behaviors have not been studied. In a step ahead, magnetic energy transfer in an ordered array of magnetostatically coupled magnetic vortices under the application of a magnetic field localized on a single element would be interesting for the application in fast spin logic [20] and magnonic crystals [21], but have not been attempted yet. In this paper, we have studied the dynamics of 1-D chains of

nanodisks in response to both local and global time-dependent magnetic fields to understand and control the magnetostatic interaction and the consequent energy transfer. A local magnetic field pulse resembles the spin torque effect produced by the spin polarized current.

II. SIMULATION

We have performed micromagnetic simulations to numerically solve the Landau Lifshitz Gilbert equation by using object oriented micromagnetic framework (OOMMF), a public domain software from the NIST website [22]. We have simulated the magnetic ground state and time evolution of magnetization in chains of Ni₈₁Fe₁₉ (permalloy) nanodisks of perfect circular shape and circles with one flat end (D-shape). Circular nanodisks are of 200 nm diameter, 40 nm thickness and the edge to edge separation between the disks were fixed as 25 nm. D-shaped nanodisks were formed by cutting 15% of its diameter at one end and the dimensions of the D-shaped nanodisks were 200 nm × 170 nm × 40 nm. Calculations were performed by dividing the samples into a two dimensional array of cells with dimensions of 5 nm × 5 nm × 40 nm. In our calculation, the linear dimensions of the cells are similar to the exchange length, which is defined as $\sqrt{(A/2\pi M_s^2)}$, where A is the exchange constant and M_s is the magnetization, respectively, and has a value of about 5 nm in permalloy. The change in relative energy error with reduced cell size below the exchange length is generally not significant compared to the increase in required computation time [23]. We choose six different unique magnetic configurations for the chain labeled as “type I,” “type II,” “type III,” “type IV,” “type V,” and “type VI” as shown in Fig. 1(a)–(f). “Type I” and “type II” correspond to opposite core polarization in alternate disks and same core polarization in each disk, respectively in a chain of circular disks. “Type III” and “type IV” correspond to the vortices of same core polarization in chains of D-shaped nanodisks arranged in same and reverse order, respectively. In “type V” D-shaped disks are arranged with the flat end at the upper and lower side of the disk in alternative disks. In “type-VI,” D-shaped disks are arranged with their flat

Manuscript received October 25, 2009; revised December 19, 2009; accepted January 06, 2010. Current version published May 19, 2010. Corresponding author: A. Barman (e-mail: abarman@bose.res.in; a_barman@yahoo.com).

Color versions of one or more of the figures in this paper are available online at <http://ieeexplore.ieee.org>.

Digital Object Identifier 10.1109/TMAG.2010.2040587

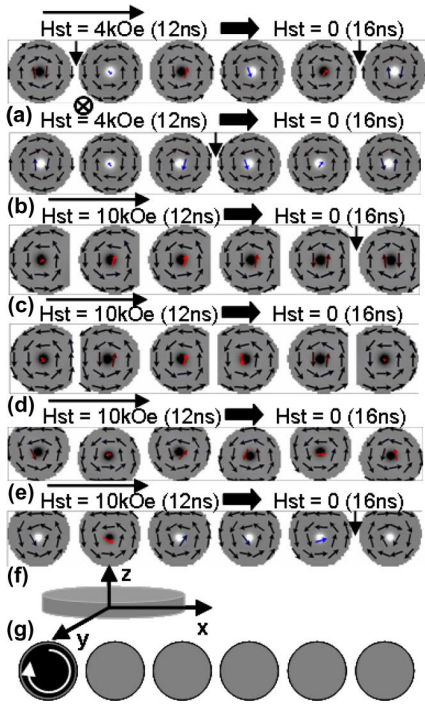


Fig. 1. Static magnetic images of chains of magnetic nanodisks showing (a) “Type I”; (b) “Type II”; (c) “Type III”; (d) “Type IV”; (e) “Type V”; and (f) “Type VI” configurations. (g) Simulation geometry for the dynamics under the application of a local rotating magnetic field. The downward arrows indicate the changes in the vortex chirality in consecutive disks.

ends always at the upper side of the disk. The simulation geometry is presented in Fig. 1(g). After applying a large static magnetic field (H_{st}) to saturate the sample, the field was reduced to zero and the magnetizations were relaxed for 16 ns with a large damping constant $\alpha = 0.5$ to damp the precession and relax the magnetization fully within the given time.

The simulations assume typical material parameters for permalloy, $4\pi M_s = 10.8$ kOe, $A = 1.3 \times 10^{-6}$ erg/cm, $H_k = 0$, and $g = 2.2$. To excite the dynamics of the vortex core, a right handed circular rotating magnetic field [14]–[17] at the resonance frequency 1.26 GHz (for type I and II) or 1.39 GHz (for type III, IV, V, and VI) and 40 mT amplitude is applied in the x – y plane to the sample. The local field is applied on the left most disk while the global field is applied uniformly on all disks of the chain. The dynamic magnetization averaged over the entire sample volume and images of the same were saved for a total duration of upto 15 ns at intervals of 10 ps. A unique damping parameter of 0.008 for permalloy was assumed in the dynamic simulation. Simulated time resolved magnetization and their corresponding FFT spectra for the local excitation are shown in Fig. 2. Comparison of the transmittance of the local excitation from disk 1 to disk 6 is presented in Fig. 3. Fig. 4 shows the energy transfer process schematically. Fig. 5 compares the dynamics of the “type IV” chain under local and global excitations. The static magnetic configurations (see Fig. 1) show that in “type I” the cores in the neighboring disks are antiferromagnetically coupled and the chirality of neighboring disks change twice as marked by downward arrows. In types II, III and VI chirality changes only once but in types IV and V, chirality is same in all disks. In “type VI” vortex cores

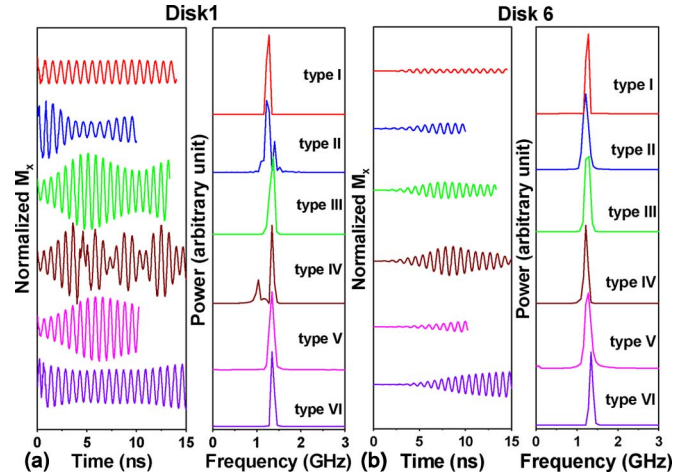


Fig. 2. Time resolved magnetization curves and corresponding FFT spectra from (a) disk 1 and (b) disk 6 of all types of 1-D chains of nanomagnets.

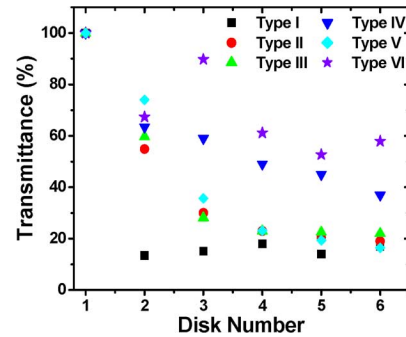


Fig. 3. Transmittance of the peak amplitude of oscillation of the gyrotropic mode is plotted as a function of the disk number.

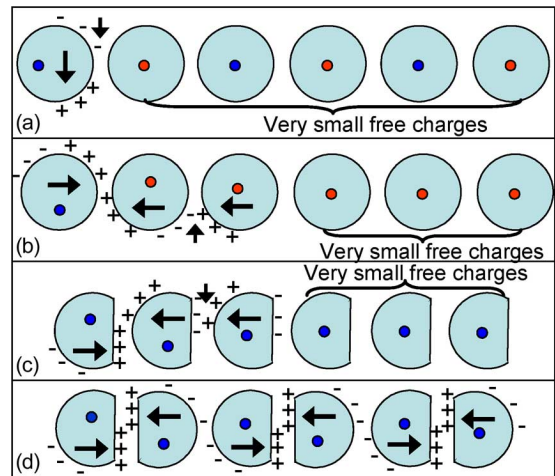


Fig. 4. Schematic showing the dynamic magnetic side charge distributions after the application of a local rotating magnetic field. The arrows inside the disks represent the free in-plane spin and the vertical arrows outside the disks indicate sharp drop in the interaction energy.

are oppositely polarized in disks 1 and 2. However, in types II, III, IV, and V chains core polarizations are same for all disks.

III. RESULTS AND DISCUSSIONS

Dynamic processes for all types of systems studied here show a gyrotropic rotational mode of the vortex core described by Thiele’s equation of motion [24]. The demagnetizing field

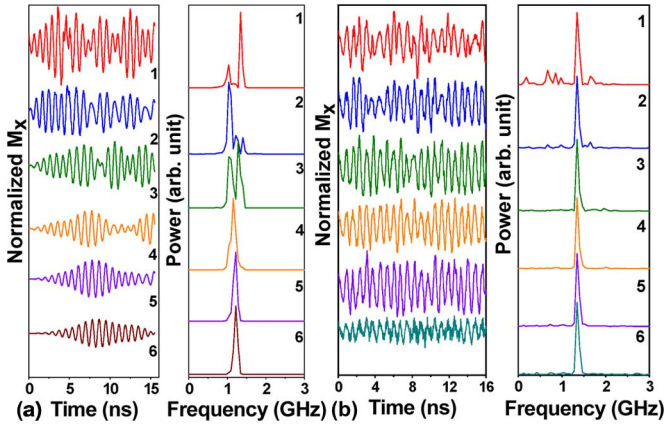


Fig. 5. Time resolved magnetization curves and corresponding FFT spectra of the “Type IV” chain under the application of (a) a local field on disk 1 of the chain and (b) a global field applied uniformly over all disks of the chain.

within each nanodisk is modified by the magnetostatic coupling between the nanodisks in the dynamic regime. Consequently, four different aspects may be observed. These are: (a) vortex core oscillations of individual nanodisks; (b) core-to-core interaction between the nanodisks in a chain; (c) interaction of vortex core with the spin waves generated within the in-plane spin configuration; and (d) the magnetostatic interaction of the in-plane spins between the nanodisks. Here, we have investigated the variation of the peak amplitude of excitation of disk 1 (master signal) under the application of identical field and the transmittance of local excitation from disk 1 to disk 6. In the FFT spectra (see Fig. 2) some additional minor peaks or peak broadening is observed probably due to the nonlinearity in the magnetic potential in which the vortex cores gyrate due to large amplitude of the rotating field and the inter-disk interactions.

The master signal is lowest in “type I” but gradually increases by a factor of 3.4 in “type IV”. For types V and VI the master signal decreases slightly but remains much higher than “type I”. Within the group of chains of same type of disks (“type I” and “type II” and types III, IV, V, and VI) this variation may be attributed to the variation in the inter-disk interaction. However, variation observed between two different groups of chains is mainly due to self magnetostatic field within the individual nanodisk. In addition, core polarizations of the neighboring disks play an important role by introducing additional interaction energy. As a result, types I and VI have lowest master signals among all types of chains due to opposite core polarizations in disks 1 and 2. On the other hand, all other types of chains have same core polarizations in all disks, and have higher master signals.

Comparison of the transmittance of local excitation from disk 1 to disk 6 through the intermediate disks for all types of chains is plotted in Fig. 3. The transmittance varies from 16% to 58% from “type I” to “type VI” chains except for a dip observed for type V, which shows about 20% transmittance. This enhanced transmittance coupled with enhanced master signal produces a large increase in the absolute amplitude of the transmitted signal in “type IV” and “type VI” chains. The observed variation in transmittance may be described in terms of the magnetostatic

coupling between the disks mediated by the in-plane spin configuration and the combination of vortex core polarization and chirality play important roles in determining the above. The interaction energy is very small in absence of any external magnetic field due to the perfect flux closure arrangement. However, on application of the local magnetic field on disk 1, the vortex core of the first disk shifts from the equilibrium position, the flux closure arrangement breaks, the magnetic side (surface) charges ($\sigma = \vec{m} \cdot \hat{n}$) appear and the inter-disk interaction mediated by these side charges causes the transfer of the gyrotropic core oscillation from disk 1 to disk 6 through the intermediate disks.

The magnetostatic energy is related only to the magnetic surface charges appearing along the envelope of the disk and is quantified as the surface integral of the product of the surface charges divided by the distance. Using this straightforward principle, we may understand the transmittance characteristics of various types of chains and their dependence on three factors, the sign and magnitude of the surface charges and the distance between those. Due to the local field excitation the vortex core oscillations in various disks in the chains start at different times and consequently they are not in phase. This determines the dynamic magnetic side charge distribution which is shown schematically in Fig. 4 for a particular instant of time. In “type-I” chain the magnetic side charges in disks 2 to 6 are very small, giving rise to very small interaction energy between disk 1 and disk 2 and to subsequent disks and consequently the transmission is very poor from disk 1 to disk 2 through to disk 6. In “type II” and “type III” chains, the opposite side charges between disks 2 and 3 causes small interaction energy between these disks and hence transmissions fall sharply. This causes very small amplitude of vortex core gyration and hence small magnetic side charges in the consequent disks and the overall transmission is low. However, in “type-IV” chain a different scenario is observed. From disk 1 to disk 6 the magnetic side charges in consecutive disks are of same sign resulting in positive interaction energy between neighboring disks, whose magnitude decreases from disk 1 to disk 6 due to the decrease in the amount of surface charges. This gives rise to a high transmission and a linear decrease in transmission from disk 1 to disk 6 in “type-IV” chain. In “type V” a similar behaviour as “type III” and in “type VI” similar behavior as “type IV” is observed and hence they are not shown in Fig. 4. In “type VI” an additional advantage of shorter separation between the magnetic side charges in all disks as opposed to “type IV” causes the increased transmittance in this type of chain.

Fig. 5 shows the time-resolved dynamics and the corresponding FFT spectra for “type IV” chain under the application of a global rotating magnetic field. Different disks in the chain have different oscillation amplitude and even slightly varying frequencies. This is due to the fact that the vortex cores of different disks are located in different magnetic potentials. For example, disk 1 and disk 6 have remarkably different dynamics compared to other disks, as they have no neighbors at their left and right side, respectively. Consequently, the magnetostatic fields on these two disks are different from other disks in the chain. Hence, the variation in the dynamics of various disks in this chain under the application of a local magnetic field is partly due to the intrinsic dynamics of the chain as observed

from their dynamics under a global field and rest is due to the energy transfer process from the excited disk to the subsequent disks.

IV. CONCLUSION

In conclusion, we have performed micromagnetic simulations to investigate the magnetic vortex dynamics in 1-D chains of nanomagnets under local and global time-dependent fields. Our simulations demonstrate that control over the shape of elements and polarization and chirality of the vortices can improve the transmittance of local excitation of one disk to the subsequent disks. The total transmitted signal also improves for the optimum design. The optimization process is a result of increased magnetostatic interaction between the disks after the time-dependent field is applied. The polarization, chirality and shape of the disks influence the sign, magnitude and separation of the magnetic side charges during the dynamics and hence by tailoring these properties the transmittance could be optimized. The combination of desired vortex polarization and chirality was obtained by varying the initial conditions for obtaining static configuration. Present study can be easily extended to two and three dimensional arrays of magnetic vortex system to create and tailor artificial band structures of magnetic excitation modes and to construct basic logic operations. A clever choice of geometric parameters of the array may result in the formation of magnonic crystals with higher energy efficiency.

ACKNOWLEDGMENT

The work of S. Barman was supported by Grant SR/FTP/PS-71/2007) from the Department of Science and Technology, Government of India.

REFERENCES

- [1] R. P. Cowburn, D. K. Koltsov, A. O. Adeyeye, M. E. Welland, and D. M. Tricker, "Single-domain circular nanomagnets," *Phys. Rev. Lett.*, vol. 83, pp. 1042–1045, Aug. 1999.
- [2] T. Shinjo, T. Okuno, R. Hassdorf, K. Shigeto, and T. Ono, "Magnetic vortex core observation in circular dots of permalloy," *Science*, vol. 289, pp. 930–932, Aug. 2000.
- [3] K. Y. Guslienko, W. Scholz, R. W. Chantrell, and V. Novosad, "Vortex-state oscillations in soft magnetic cylindrical dots," *Phys. Rev. B*, vol. 71, pp. 144407-1–144407-8, Apr. 2005.
- [4] X. Zhu, Z. Liu, V. Metlushko, P. Grütter, and M. R. Freeman, "Broadband spin dynamics of the magnetic vortex state: Effect of the pulsed field direction," *Phys. Rev. B*, vol. 71, pp. 180408-1–180408-4, May 2005.
- [5] K. Y. Guslienko, X. F. Han, D. J. Keavney, R. Divan, and S. D. Bader, "Magnetic vortex core dynamics in cylindrical ferromagnetic dots," *Phys. Rev. Lett.*, vol. 96, pp. 067205-1–067205-4, Feb. 2006.
- [6] V. Novosad, M. Grimsditch, K. Y. Guslienko, P. Vavassori, Y. Otani, and S. D. Bader, "Spin excitations of magnetic vortices in ferromagnetic nanodots," *Phys. Rev. B*, vol. 66, pp. 052407-1–052407-4, Aug. 2002.
- [7] J. P. Park, P. Eames, D. M. Engebretson, J. Berezovsky, and P. A. Crowell, "Imaging of spin dynamics in closure domain and vortex structures," *Phys. Rev. B*, vol. 67, pp. 020403-1–020403-4, Jan. 2003.
- [8] R. Hertel, S. Gliga, M. Fähnle, and C. M. Schneider, "Ultrafast nanomagnetic toggle switching of vortex cores," *Phys. Rev. Lett.*, vol. 98, pp. 117201-1–117201-4, Mar. 2007.
- [9] K. Y. Guslienko, K. Lee, and S. Kim, "Dynamic origin of vortex core switching in soft magnetic nanodots," *Phys. Rev. Lett.*, vol. 100, pp. 027203-1–027203-4, Jan. 2008.
- [10] B. Van Waeyenberge, A. Puzic, H. Stoll, K. W. Chou, T. Tylliszczak, R. Hertel, M. Fähnle, H. Brückl, K. Rott, G. Reiss, I. Neudecker, D. Weiss, C. H. Back, and G. Schütz, "Magnetic vortex core reversal by excitation with short bursts of an alternating field," *Nature*, vol. 444, pp. 461–464, Sep. 2006.
- [11] Q. F. Xiao, J. Rudge, B. C. Choi, Y. K. Hong, and G. Donohoe, "Dynamics of vortex core switching in ferromagnetic nanodisks," *Appl. Phys. Lett.*, vol. 89, pp. 262507-1–262507-3, Dec. 2006.
- [12] S. Choi, K. S. Lee, K. Y. Guslienko, and S. K. Kim, "Strong radiation of spinwaves by core reversal of a magnetic vortex and their wave behaviors in magnetic nanowire waveguides," *Phys. Rev. Lett.*, vol. 98, pp. 087205-1–087205-4, Feb. 2007.
- [13] K. Yamada, S. Kasai, Y. Nakatani, K. Kobayashi, H. Kohno, A. Thiaville, and T. Ono, "Electrical switching of the vortex core in a magnetic disk," *Nature Mater.*, vol. 6, pp. 269–273, Mar. 2007.
- [14] V. P. Kravchuk, D. D. Sheka, Y. Gaididei, and F. G. Mertens, "Controlled vortex core switching in a magnetic nanodisk by a rotating field," *J. Appl. Phys.*, vol. 102, pp. 043908-1–043908-4, Aug. 2007.
- [15] M. Curcic, B. Van Waeyenberge, A. Vansteenkiste, M. Weigand, V. Sackmann, H. Stoll, M. Fähnle, T. Tylliszczak, G. Woltersdorf, C. H. Back, and G. Schutz, "Polarization selective magnetic vortex dynamics and core reversal in rotating magnetic fields," *Phys. Rev. Lett.*, vol. 101, pp. 197204-1–197204-4, Nov. 2008.
- [16] S. K. Kim, K. S. Lee, Y. S. Yu, and Y. S. Choi, "Reliable low-power control of ultrafast vortex-core switching with the selectivity in an array of vortex states by in-plane circular-rotational magnetic fields and spin-polarized currents," *Appl. Phys. Lett.*, vol. 92, pp. 022509-1–022509-3, Jan. 2008.
- [17] K. S. Lee and S. K. Kim, "Two circular-rotational eigenmodes and their giant resonance asymmetry in vortex gyrotropic motions in soft magnetic nanodots," *Phys. Rev. B*, vol. 78, pp. 014405-1–014405-6, Jul. 2008.
- [18] J. Shibata, K. Shigeto, and Y. Otani, "Dynamics of magnetostatically coupled vortices in magnetic nanodisks," *Phys. Rev. B*, vol. 67, pp. 224404-1–224404-5, Jun. 2003.
- [19] K. S. Buchanan, P. E. Roy, M. Grimsditch, F. Y. Fradin, K. Y. Guslienko, D. D. Bader, and V. Novosad, "Soliton-pair dynamics in patterned ferromagnetic ellipses," *Nature Phys.*, vol. 1, pp. 172–176, Dec. 2005.
- [20] M. P. Kostylev, A. A. Serga, T. Schneider, B. Leven, and B. Hillebrands, "Spin-wave logical gates," *Appl. Phys. Lett.*, vol. 87, pp. 153501-1–153501-3, Oct. 2005.
- [21] Y. V. Gulyaev, S. A. Nikitov, L. V. Zhivotovski, A. A. Klimov, P. Tailhades, L. Presmanes, C. Bonningue, C. S. Tsai, S. L. Vysotski, and Y. A. Filimonov, "Ferromagnetic films with magnon bandgap periodic structures: Magnon crystals," *JETP Lett.*, vol. 77, pp. 567–570, May 2003.
- [22] M. Donahue and D. G. Porter, OOMMF User's Guide, Version 1.0 National Institute of Standard and Technology, Gaithersburg, MD, Interagency Report NISTIR 6376, 1999. [Online]. Available: <http://math.nist.gov/oommf>
- [23] A. Barman and S. Barman, "Dynamic dephasing of magnetization precession in arrays of thin magnetic elements," *Phys. Rev. B*, vol. 79, pp. 144415-1–144415-9, Apr. 2009.
- [24] A. A. Thiele, "Steady-state motion of magnetic domains," *Phys. Rev. Lett.*, vol. 30, pp. 230–233, Feb. 1973.